Capacitive response of nanoporous HMDSO film coated interdigited electrodes towards VOCs molecules

K. Dallah[a,*], A. Bellel[a], O. C. Lezzar[a], S. Sahli[b]
[a]*Laboratory of Electronic Materials Study for Medical Applications, Faculty of Technical Sciences, University of Constantine 1, Constantine 25000, Algeria.*
[b]*Laboratory of Microsystems and Instrumentations, Faculty of Technical Sciences, University of Constantine 1, Constantine 25000, Algeria.*

In this paper, nano-porous thin films capacitive-type sensors have been fabricated for the detection of volatile organic compounds (VOCs) using the micro sized interdigitated electrodes (IDEs). The sensitive layers were elaborated from hexamethyldisiloxane (HMDSO) using plasma enhanced chemical vapor deposition (PECVD) technique. The choice of HMDSO polymer as sensitive layer is based on its low dielectric constant compared to analytes ones. The sensing performances of plasma polymers were strongly correlated to their chemical and physical properties, which depend directly on the plasma polymerization conditions including monomer pressure. The sensor sensitivity was at its highest value of 0.32, 0.24 and 0.20 pF/ppm towards methanol, ethanol and acetone, respectively, for the device fabricated with the smallest gap (36 µm) and higher monomer pressure (50 Pa). Chemical and morphological structures of the elaborated thin sensitive layers have been investigated by Fourier transform infrared spectroscopy (FTIR) and atomic force microscopy (AFM) and scanning electron microscope (SEM), respectively.

(Received December 21, 2022; Accepted February 24, 2023)

Keywords: Organosilicon films, HMDSO, PECVD, Interdigitated electrodes, Capacitive sensor, Volatile organic compounds

1. Introduction

Volatile organic compounds (VOCs) are a group of chemical products in liquid form, which evaporate easily at room temperature. During the last few decades, the detection of VOCs has attracted an increasing research attention for environmental protection, human health care, industrial processing and air quality control [1]. High concentration exposure to some VOCs over a short or long term may cause diseases or serious irreversible effect. Each VOC has its own toxicity and potential for causing different health effects [2-4]. Several major environmental safety agencies, have established guidelines to limit the exposure of humans to VOCs because of their harmful effects on health, even at low concentrations [5]. VOCs do not only harm the human health but also pollute the environment. According to the World Health Organization, there are more than 4.2 million deaths every year because of air pollution [6]. Consequently, the identification and monitoring of VOCs have become serious tasks in many countries of the world and are important for the early control of environmental pollution. To achieve the goal for chemical sensor with satisfactory sensitivity, rapid response, good stability and reliability, several transduction techniques have been reported, such as resistive [7], capacitive [8], gravimetric [9] and surface Plasmon resonance [10]. These methods have shown very good results in terms of sensitivity and affinity towards different type of VOCs molecules.

However, chemocapacitors type of transduction have attracted considerable research interest in terms of processability, because they have low fabrication cost, can operate at ambient temperature (simplifying their operation), consume very small amount of energy and can easily integrated with the read-out electronics. Capacitive gas sensors consist of interdigital electrodes (IDEs) transducers coated with an appropriate sensing layer (mainly polymers) acting as analytes

* Corresponding author: khalid.dallah@umc.edu.dz
https://doi.org/10.15251/DJNB.2023.181.279

receptors. During interaction with analyte vapors, the geometrical (volume) and electrical (dielectric constant) properties of the sensing material change, inducing proportional modification in the whole sensor capacitance [11]. At present, a great variety of polymers layers have been used as sensitive coating especially for monitoring environmental pollutants, because they have rapid adsorption and desorption process at room temperature [12, 13]. For the synthesis of sensitive layers, different deposition techniques have been reported, including methods based on sol–gel [14], spin coating [15] and electrochemical deposition [16], but there are very few works reported in the literature investigating VOCs sensing properties of films deposited by plasma enhanced chemical vapor deposition technique (PECVD). There is an importance in using plasma polymerized films as sensitive coatings in chemical sensors, because they can be deposited on any substrate and feature excellent mechanical, thermal and chemical stability [17]. The sensing characteristics of plasma polymers are strongly correlated to their chemical and physical properties [18], which depend directly on the precursor nature and on the plasma polymerization conditions, including discharge powers and monomer flow rate [19]. In addition to sensing layer properties, the IDEs geometry had crucial influence on the response of the capacitive gas sensor and played an important role in the performance of the sensor towards a specific analyte [20].

In this study, PECVD technique has been used to elaborate IDEs sensitive coating from the polymerization of hexamethyldisiloxane (HMDSO). This compound (liquid under ambient conditions) has a vapor pressure of 2000 Pa at 20 ℃ favoring its application in the PECVD process. In addition, HMDSO is easily manipulated, non-toxic and inexpensive. Among the various plasma parameters, which have effects on the synthesized film structure, the monomer flow rate is fundamental. In fact, this parameter is associated with the monomer molecule fragmentation degree and radical concentration in the plasma reactor [21].

The capacitance of a typical parallel plate electrode capacitive-type sensor can be expressed as $C = \varepsilon_0 \varepsilon_{layer} A/W$, A is the electrode area, w is the gap between electrodes and ε_{layer} is the dielectric constant of the polymer film. In capacitive measurements, the detection mechanism is based on the relative change in the dielectric properties of the sensing layer upon physisoption of analyte vapor. Therefore, the dielectric constant of the mixture is directly related to the dielectric constant of the sensing layer and the analyte one. The magnitude of the corresponding capacitance change of the sensor depends on the concentration of physisorbed VOCs molecules in combination with the difference between the dielectric constants of polymer and analyte. In this work, the sensing layer deposited in HMDSO plasma has dielectric constant of about 3.1 [22], and the testing gases have a constant dielectric of 32.8, 24.5 and 21 for methanol, ethanol and acetone, respectively. Thus, due to the high dielectric constant of VOCs molecules compared to low dielectric constant of the polymer, capacitive-type sensors based on HMDSO films would be suitable for VOCs detections. In additions, porous films can be suitable for sensor response improvement and have been a subject of research over the last decade. Recently, SiOCH thin films have been synthesized by plasma polymerization of HMDSO, resulting in porous structures with low refractive index [23]. Generally, capacitive gas sensors suffer from low sensitivity due similar dielectric constants of polymer and VOCs [24]. In this study, the porous structure and low dielectric constant of the elaborated HMDSO polymers may be a technological issue for improving sensor response characteristics.

Since the gap between electrodes can have a strong influence on the sensitivity, the effect of gap spacing on the sensor response performance has been also investigated. The interdigitated capacitances (IDC) fabricated from Al electrodes were deposited on glass substrate then patterned using conventional microelectronic processes in order to form a 4-IDC sensor array [25]. Chemical properties of the elaborated thin sensitive layers were investigated by Fourier transform infrared spectroscopy (FTIR). Atomic force microscopy (AFM) and scanning electron microscope (SEM) have been used to investigate surface morphology properties. The gas sensing properties of the coated IDEs sensors have been evaluated towards different concentrations of ethanol, methanol and acetone ranging from 100 ppm to 400 ppm.

2. Experimental detail

2.1. Synthesis of HMDSO layers

Thin sensitive materials were deposited using plasma enhanced chemical vapor deposition at low frequency power from pure vapor of HMDSO. Several deposition processes of HMDSO layers were carried out at various monomer pressure in order to investigate their influence on the chemical and physical properties of the deposited films. Monomer pressure is a crucial factor since it has a strong impact on the intrinsic plasma parameters. S. M. Amanda et al, reported on organosilicon films deposited in low-pressure plasma from HMDSO, that the change in surface structure is related to the effect of the gas pressure on the collision rate fragmentation degree and on the type of functional groups generated in the plasma phase [26]. The increase of the monomer pressure reduces the mean free path of the plasma species. This variation may induce a growth in the sizes of the plasma fragments and consequently in the final surface roughness. The plasma reactor setup and polymerization process are describe elsewhere [27]. Prior to plasma coating, silicon substrates and IDEs were cleaned with methanol and acetone in ultrasonic bath for 10 min, then washed with distilled water and dried at ambient air. The film thickness has been evaluated using the optical ellipsometry (SpecEL-2000-VIS) system. The film thickness of the sensor was in the range of 360 nm–580 nm.

2.2. Characterization methods

The chemical structure of the IDEs coating films was characterized by FTIR spectroscopy. All spectra were acquired in absorbance mode in the 400–4000 cm^{-1} range using a Nicolet Avatar 360 FTIR spectrometer. Contact angle measurements were carried out at room temperature and atmospheric pressure. A water drop of 5 µl was deposited onto the coated IDEs surface using a micro-syringe. The drop image was acquired by a numerical camera, then transmitted to a computer for contact angle evaluation. The layer surface roughness was examined on a nanometer scale using atomic force microscopy. AFM images were recorded in tapping mode (resonance frequency 330 kHz) in air at room temperature using Angstrom Advanced (AA2000, USA) instrument. All scans are characterized by measuring the root mean square roughness (Rms). Additionally, the scanning electron micrograph (SEM) of the polymer film was obtained using JEOL-Jed 2300.

2.3. Fabrication of IDE

The interdigitated electrode transducers were fabricated from Al electrodes deposited on glass substrate using conventional microelectronic processes. A 100 nm thick aluminum layers deposited in clean room on glass substrates by thermal evaporation technique are patterned using standard photolithography and lift-off process [28]. The geometrical characteristics of the sensor are the nominal width of each finger w and the distance between adjacent fingers g [metallization ratio $\eta = w/(w+g)$, spatial wavelength $\lambda = 2(w+g)$. Each IDC sensor covers an area of 18 mm x 18 mm, with a total number of fingers N = 80. In order to investigate the effect of the interdigital electrode gap on the performance of the studied capacitive sensor, four different gaps spacing (36 µm, 80 µm, 200 µm and 400 µm) were fabricated.

2.3. Gas sensing measurements

Chemical sensing properties of the studied sensor were evaluated towards methanol, ethanol and acetone molecules. All sensing measurements were carried out in a homemade chamber (a sealed Pyrex glass chamber of 1L volume) with precisely controlled temperature and atmosphere. The experimental setup used for VOCs sensing measurement is illustrated in Figure 1.

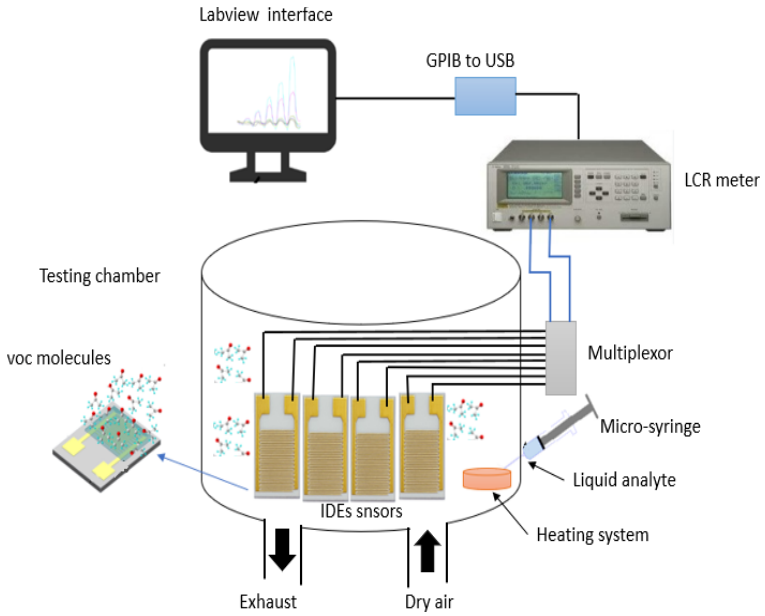

Fig. 1. Schematic representation of the testing chamber.

A liquid of known volume and density was introduced in the testing chamber using a micro-syringe and allowed to evaporate freely on a hotplate placed inside the testing chamber. The capacity change of the sensors upon exposure to the VOCs vapors was monitored by a programmable LCR meter (Hewlett Packard 4284A). Generally, polymer dielectric constants are frequency-dependent. S. Zeinali et al [29] reported that sensors had more capacitive response under lower frequencies but with no reliable and repeatable responses. At higher frequencies, the studied sensors showed more reliable and repeatable responses and better linearity. Therefore, the capacitances of IDE-based sensors were tested as a function of VOCs concentration by a LCR meter analyzer at the operation frequency of 10 kHz. Before measurements, the sensor was allowed to stabilize in dry air environment to achieve baseline stabilization (stable capacitance value). After the capacitance change reached steady state, the sensor was exposed to dry air for baseline recovery. The concentrations of each VOC were varied in the range of 100–400 ppm. The temperature of the sensor was kept at room temperature with the help of temperature controller.

3. Results and discussions

3.1. Chemical and physical characterizations

Water contact angle values measured on plasma polymerized HMDSO surface were in the order of 84°, 88°, 94° and 130°, respectively for films elaborated at monomer pressure of 20, 30, 40 and 50 Pa. These measured contact angle values indicating the transformation of the polymer surface properties from hydrophobic behavior to highly hydrophobic. The FTIR spectra used to characterize the chemical structures of the plasma polymerized HMDSO films elaborated at monomer pressure of 20, 30, 40 and 50 Pa are shown in Figure 2, respectively.

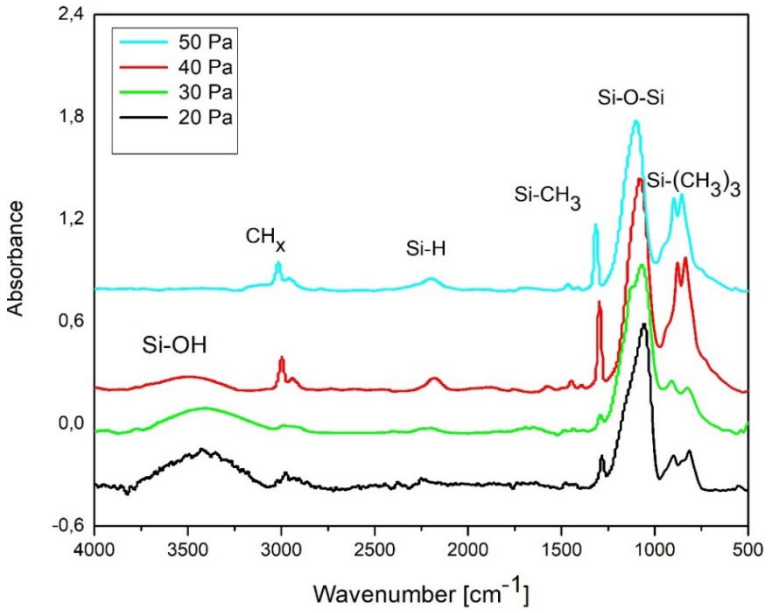

Fig. 2. FTIR spectra of HMDSO films plasma polymerized at different monomer pressure.

According to literature [30], when the plasma polymerization is performed in pure vapor of HMDSO, the infrared spectra exhibit a broad band between 950 and 1250 cm^{-1} corresponding to Si–O–Si. The peak position of Si-O-Si band slightly shifts toward lower wave numbers which can be related to the change in bonding [31]. The spectrum shows strong peaks of the methyl groups $Si-CH_3$ at around 840 cm^{-1}characteristic for polymer with low degree of crosslinking. A small contribution due to Si-H bonds can be observed at 2240 cm^{-1}. In addition, FTIR spectra show the presence of CH_x peaks at around 2972 cm^{-1}. CH_x peak intensity is more pronounced for film deposited at higher pressure of HMDSO precursor (50 Pa). It is reported that film becomes more porous and low dense due to the presence of high CH_x proportion [32, 33]. Films deposited at low vapor pressure of HMDSO revealed the presence of surface hydroxyl band (Si-OH) situated between 3100 and 3600 cm^{-1}. However, Si-OH bonds are not detected for the film deposited at higher pressure. This is in good agreement with the high hydrophobic behavior of HMDSO film surface with water contact angle higher than 130°. It would be expected that IDE sensor coated with hydrophobic film could detect volatile organic compounds with decreasing humidity effect from ambient conditions.

Atomic force microscopy has been used to examine the surface morphology of the IDEs coatings. Figure 3 a, b, c and d show high resolution AFM images (2 μm × 2 μm) recorded on the surface of plasma polymerized films from pure vapor of HMDSO at a pressure of 20, 30, 40 and 50 Pa, respectively.

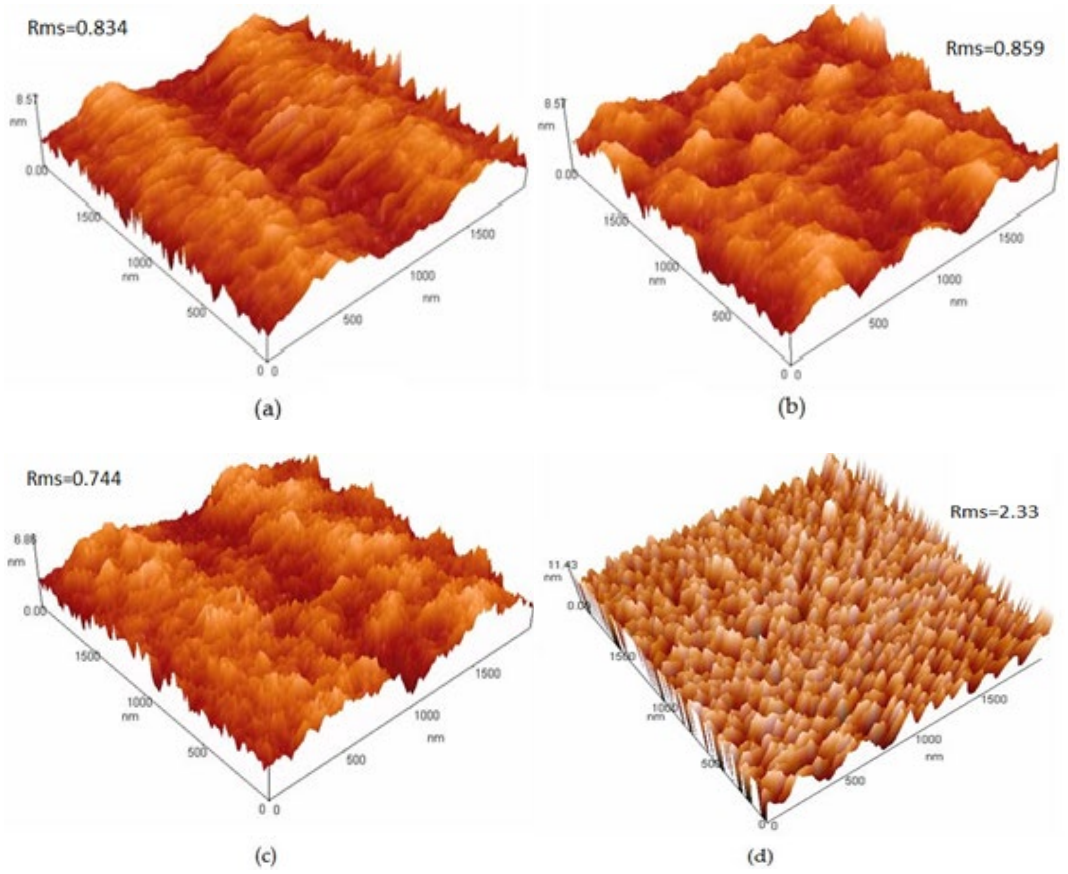

Fig. 3. AFM images of HMDSO films elaborated at different monomer pressure: (a) 20 Pa, (b) 30 Pa, (c) 40 Pa and (d) 50 Pa.

The surface topography consists of a relatively uniform sea-island structure. For layers elaborated at lower monomer pressure, AFM scans show that coatings have a comparatively smooth and homogeneous surface. No big difference can be detected regarding the root mean square roughness (Rms=0.744 nm) of the layers, which was averaged from three individual scans. The increase in the monomer pressure (50 Pa) results in relatively rougher surface (Rms=2.33 nm). The increase in surface roughness leads to the increase in the specific surface area (surface to volume ratio). The enhanced sensor surface area can then accommodate more adsorption sites, which justifies the enhanced adsorptive properties of IDEs based senor coated at higher monomer pressure. The higher surface roughness could be caused by number of reactions taking place in the plasma phase. The increase of monomer pressure decreases the mean free path of moving reactive and neutral species, which increases the number of collisions in the plasma. M. Jaritz et al [30] reported that if reactive species carry out many collisions or reactions until reaching the substrate surface, could increase the deposition rate and the layer roughness as well as they can change the layer's chemical composition. The porous structure of the IDEs coating has also been characterized by scanning electron microscope. Figure 4 illustrates the micro surface morphology of the HMDSO coating at high monomer pressure (50 Pa). SEM image shows a sponge-like nano-porous structure with pore size in the range of about 50-100 nm randomly distributed over the film surface. The plasma polymerized film has many nano-sized pores, giving it a large surface area for absorbing VOC vapor.

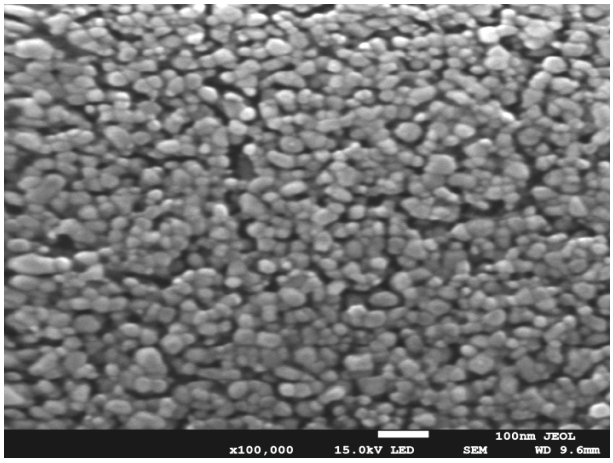

Fig. 4. SEM image of HMDSO film elaborated at 0.5 mbar.

3.2. Sensor response evaluation

The sensing mechanism of the studied IDEs-based sensors rely on the film absorption of analyte molecules accompanied by the modifications in the dielectric properties and/or thickness (polymer swelling) of the sensing layer, which alter the capacitance of the device [34]. We evaluate capacitive responses as changes in sample capacitance $\Delta C = C_{gas} - C_{air}$. The initial capacitance values were in the order of 12.7, 13.5, 13.7 and 14.8 pF for IDE-based sensor coated at 20, 30, 40, and 50 Pa, respectively. The dynamic responses of IDE-based sensors upon exposure to VOC molecules followed by dry air purging are shown Figures 5 a, b, c, and d for thin layer plasma polymerized from pure vapor of HMDSO at monomer pressures of 20, 30, 40, and 50 Pa, respectively.

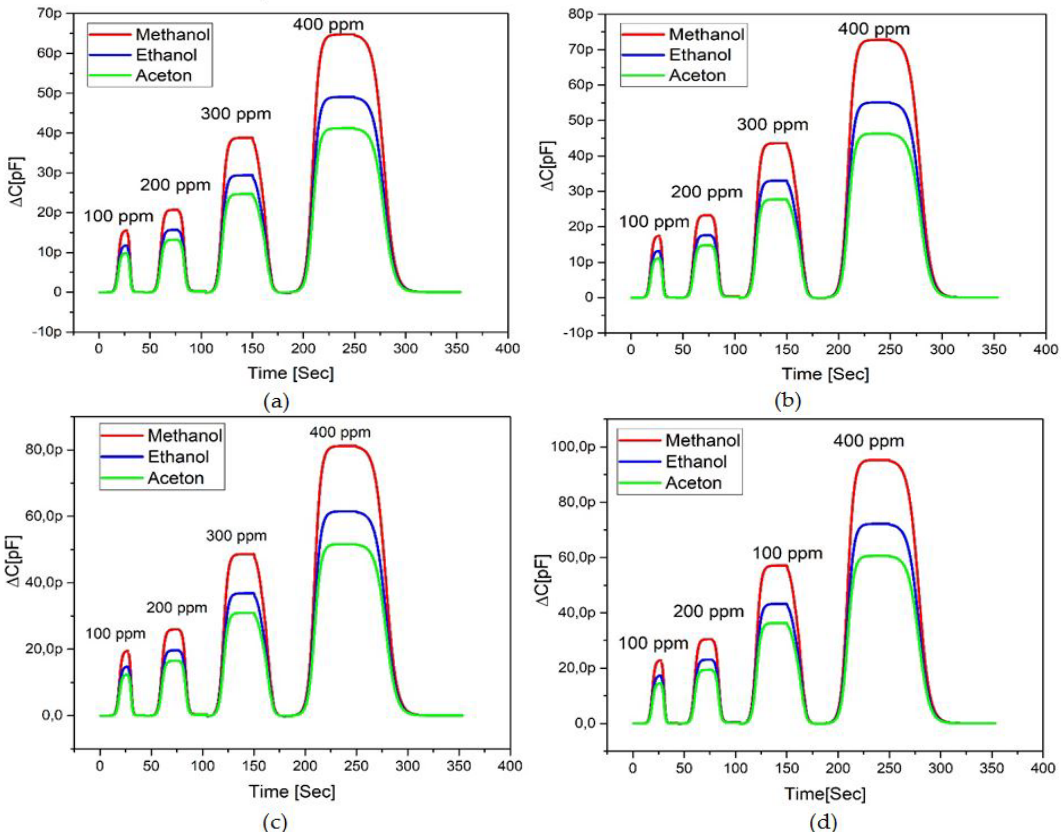

Fig. 5. Dynamic capacitance response of the sensors to VOC molecules for HMDSO films deposited at: (a) 20 Pa, (b) 30 Pa, (c) 40 Pa and (d) 50 Pa.

The sensor responses in terms of capacitance change were plotted against time for concentrations of ethanol, methanol and acetone vapors ranging from 100 to 400 ppm. All polymers coating exhibit higher response to VOC molecules, due to their high dielectric constant in comparison to the dielectric constants of the polymer sensing layer (3.1). The high capacitance change indicates significant variation in effective dielectric constant of the film even for low ppm range. The kinetic response showed that the absolute value of the ΔC increases gradually with time then reaches a steady-state value. The back returning of the sensor to its baseline value was taken as indication of full desorption of analytes from the coated electrode surface. For lower concentration of organic molecules, high surface area porous film is partially filled causing less change in effective dielectric constant. However, when concentration increases, more molecules will be physisorbed causing large change in effective dielectric constant of the sensor according to the following Clausius–Mossotti mixing rule [35].

$$\frac{\varepsilon_{mix}-1}{\varepsilon_{mix}+2} = \frac{\varepsilon_a-1}{\varepsilon_p+2}\,(1-\Phi_s)\,\frac{\varepsilon_a-1}{\varepsilon_p+2}\,\Phi_s \qquad (1)$$

where: ε_p, ε_a and are the dielectric constants of polymer and analyte, respectively, ε_{mix} is the new permittivity value and Φ_s is the volume fraction of the analyte molecules in the polymeric film. The large change in dielectric constant leads to an increase in sensor capacitance value. Response and recovery time are important parameters for estimating the sensor performance. The time taken by the sensor to achieve 90% of the total ΔC is defined as the response time and the recovery time for the return to 0%. The studied sensor takes very little time (about 12 s) to reach the equilibrium in response to the step change of VOC concentration. The recovery time of the sensor is also very small (about 19 s) indicating fast desorption of organic molecules from the polymer pores.

Figure 6 shows the variations of the capacitance change ΔC as a function of analyte concentration, plotted using saturated values of the sensor responses. For all type of sensor, the equilibrium ΔC values increase with increasing VOC concentration. Sensor coated at high monomer pressure exhibits the best sensitivity compared to IDEs-based sensor elaborated at lower monomer pressure and confirm the relation between chemical and physical structures of the films and their sensing properties. As an example, for 50 Pa polymers, the sensor capacitance change was 95, 72 and 60 pF for 400 ppm level of methanol, ethanol and acetone, respectively, while for 20 Pa sensors, the capacitance change was in the order of 64, 49 and 41 pF, respectively. The higher sensing properties of 50 Pa polymer correlates well with the FTIR and SEM results, which show a porous and highly hydrophobic surface structure. Figure 6 shows that the VOC sensing behavior of the deposited film is linear after the analyte concentration of 200 ppm, following equation $y = 0.32x-36.27$, with a linear fit of $R^2 = 0.989$. VOC levels above 200 ppm have a considerable effect on the sensitivity due to porous nature of the IDEs coating. The results also show that IDE-based sensors were more sensitive to methanol vapor than other organic vapors (Fig. 6). The responses are in the following descending order: methanol ($\varepsilon_r = 32.8$)> ethanol ($\varepsilon_r = 24.5$)> acetone ($\varepsilon_r = 21$). The size of analyte molecules is another factor influencing the sensor response. Smaller molecules are more able to diffuse inside the polymer matrix and get absorbed. The results of figure 6 indicate that for the same analyte concentration, ΔC increaseswith decreasing molecular sizean increasing dielectric constant of analyte. As an example, methanol induces a higher ΔC due to its lower molecular size and higher dielectric constant. Smaller molecules diffuse easily through the polymer surface pores and the higher constant value induces a large change in sensor capacitance according to Clausius–Mossotti mixing rule. Unlike methanol and ethanol molecules, acetone has lower dielectric constants and are a bigger molecule (more difficult to get absorbed). Due to these two factors sensors responses towards acetone are lower as seen in Figure 6.

In general, the sensing mechanisms for the capacitive-type sensor can be attributed to the physisorption of analyte species inside the sensing layer matrix. This leads to the change of ΔC due to the change of the sensing layer permittivity $\frac{\partial C}{\partial \varepsilon_{mix}}\Delta\varepsilon_{mix}$ and to sensing layer swelling $\frac{\partial C}{\partial h}\Delta h$ as analyte molecules diffuse within the polymer matrix. Accordingly, the response of the

sensor is the sum of these two responses contribution [36].

$$\Delta C = \frac{\partial C}{\partial \varepsilon_{mix}} \Delta \varepsilon_{mix} + \frac{\partial C}{\partial h} \Delta h \tag{2}$$

where: h is the sensing layer thickness and ε_{mix} is new dielectric constant of film

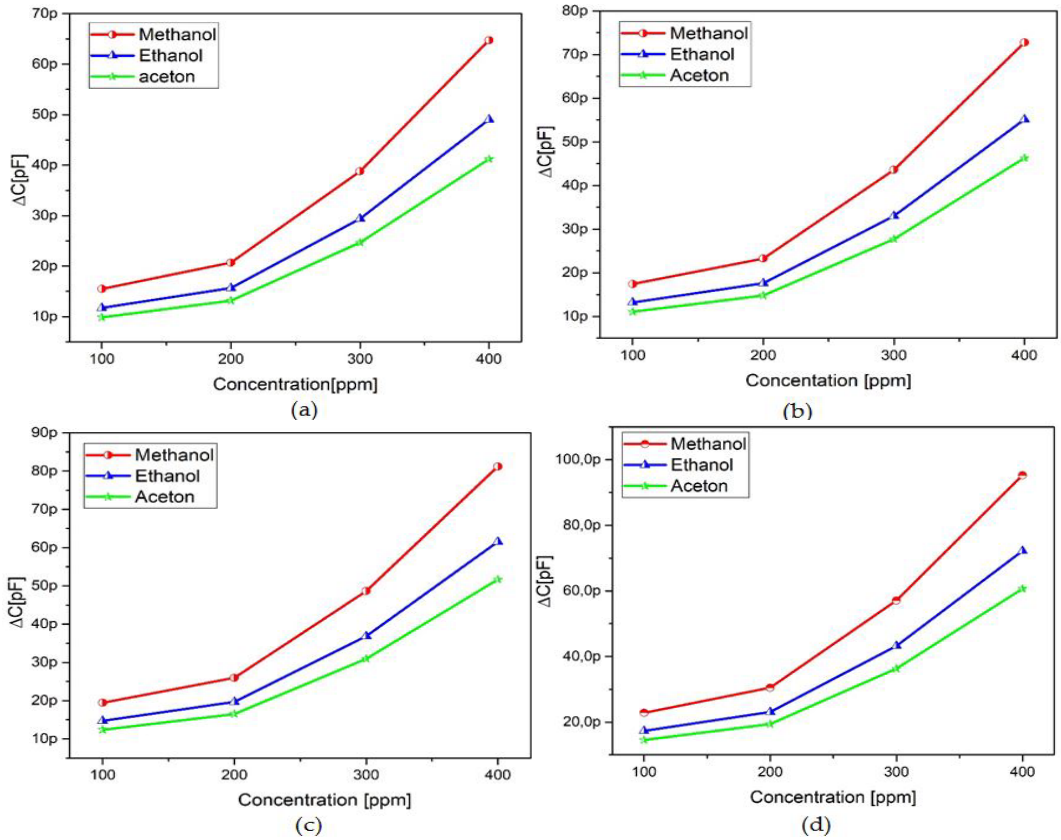

Fig. 6. Capacitance change versus VOCs concentrations for film deposited at: (a) 20 Pa, (b) 30 Pa, (c) 40 Pa and (d) 50 Pa.

The effect of polymer swelling has been studied by Igreja and Dias [37, 38]. They have suggested that when the dielectric constant of the analyte is much higher than the dielectric constant of the sensing layer, the contribution of swelling to the total capacitance change ΔC is small and the response of the sensor is dominated by the change of the permittivity of the sensing layer. In this study, the dielectric constant of the elaborated sensing layer is in the order of 3.1, which is much lower than the dielectric constant values of methanol, ethanol and acetone (32.8, 24.5 and 21, respectively). Thus, the sensor response is dominated by the IDE coating layer permittivity change rather than polymer swelling.

The sensitivity s of the sensors is defined as the ratio of change in capacitance ΔC to the change in VOC molecule concentration (Δppm). The sensitivity and limit of detection (LOD) of the investigated sensors to methanol, ethanol and acetone vapors are summarized in table 1. LOD is defined by the ratio of $3\sigma/s$ .Where σ is the noise level of the fabricated IDE sensor (estimated at 0.2 pF) and s is the sensor sensitivity to a specific analyte. Sensor coated at high monomer pressure (50 Pa) has the greatest sensitivity to VOC molecules compared to IDE-based sensor coated at low monomer pressure. The sensitivity towards methanol, ethanol and acetone was found to be 0.32, 0.24 and 0.20 pF/ppm, respectively. These values are very good compared to other capacitive type sensor [39-41] and can be easily measured by the interface electronics circuit. Concerning the LOD, the sensors coated at 50 Pa presents a lower detection limit. They can detect up to 1.8, 2.5 and 3 ppm of methanol, ethanol and acetone, respectively.

Table 1. The sensitivity and limit of detection for IDE-based sensor coated at different monomer pressure.

	20 Pa		30 Pa		40 Pa		50 Pa	
	Sensitivity [pF/ppm]	LOD [ppm]	Sensitivity [pF/ppm]	LOD [ppm]	Sensitivity [pF/ppm]	LOD [ppm]	Sensitivity [pF/ppm]	LOD [ppm]
Methanol	0.22	2.7	0.24	2.5	0.28	2.14	0.32	1.87
Ethanol	0.17	3.52	0.19	3.15	0.21	2.85	0.24	2.5
Aceton	0.14	4.3	0.16	3.75	0.17	3.52	0.20	3

3.3. Effect of gap spacing

In order to investigate the effect of interdigital electrode gap (w) on the performance of VOC sensor, different kindsof w were patterned on glass substrates (36 µm, 80 µm, 200 µm and 400 µm). All the inter-digital electrodes have the same length of 18 mm. Table 2 summarizes the sensing parameters of the four IDEs sensors plasma coated at monomer pressure of 50PA and evaluated towards VOCs molecules with concentration ranging from 100 to 400 ppm. It has been shown that sensor with $w = 36$ µm recorded the highest sensitivity and lowest limit of detection compared to others IDEs-based sensors. The experimental results showed that the device with the shortest electrode gap produced the best sensitivity than longer gaps. This behavior has also been found by other workers [42, 43]. The capacitance C is inversely proportional to the gap between the electrodes, it is expected that the highest capacitance response is obtained from the smallest gap of device as shown in Table 2.

Table 1. The sensitivity and the limit of detection for IDE-based sensor with different gap spacing.

	36 µm		80 µm		200 µm		400 µm	
	Sensitivity [pF/ppm]	LOD [ppm]	Sensitivity [pF/ppm]	LOD [ppm]	Sensitivity [pF/ppm]	LOD [ppm]	Sensitivity [pF/ppm]	LOD [ppm]
Methanol	0.32	1.87	0.15	4	0.024	25	0.012	50
Ethanol	0.24	2.5	0.12	5	0.020	30	0.010	60
Aceton	0.20	3	0.11	5.45	0.019	31.57	0.019	64.51

4. Conclusions

Capacitive type sensors were fabricated using a dielectric layer made from the plasma polymerization of HMDSO at different monomer pressure. The variation of the plasma polymerization parameter resulted in different VOC sensing properties which were correlated to the results of the film characterization by FTIR, contact angle measurements and SEM photography. The VOCs sensing results were interpreted by considering the presence of nonporous structure and high specific surface area associated with super-hydrophobicity. For the device fabricated with the smallest gap (36 µm) and higher monomer pressure (50 Pa), the sensor sensitivity was at its highest value of 0.32, 0.24 and 0.20 pF/ppm towards methanol, ethanol and acetone, respectively.

All fabricated sensors have good affinity towards methanol vapors due to their lower molecules size and higher dielectric constant. The performance of the studied sensors in terms of sensitivity and LOD values, derived from the measurements at various analytes concentrations, indicates that the sensor shows improved response characteristics in comparison to the sensors reported in the literature and has the potential to be applied for the detection of VOCs.

References

[1] W.-T. Tsai, Environments, vol. 3, no. 3, p. 23, 2016; https://doi.org/10.3390/environments3030023

[2] H. Onthath et al., Macromolecular Symposia, 2021, vol. 400, no. 1, p. 2100202: Wiley Online Library; https://doi.org/10.1002/masy.202100202

[3] S. Khan, S. Le Calvé, and D. Newport, Sensors and Actuators A: Physical, vol. 302, p. 111782, 2020; https://doi.org/10.1016/j.sna.2019.111782

[4] V. Soni, P. Singh, V. Shree, and V. Goel, Air pollution and control: Springer, 2018, pp. 119-142; https://doi.org/10.1007/978-981-10-7185-0_8

[5] S. K. Ayyala, J. H. Tsang, C. Blackman, and J. A. Covington, 2020 IEEE SENSORS, 2020, pp. 1-4: IEEE; https://doi.org/10.1109/SENSORS47125.2020.9278881

[6] G. Korotcenkov, Handbook of gas sensor materials, Conventional approaches, vol. 1, 2013; https://doi.org/10.1007/978-1-4614-7165-3_1

[7] C. Li, P. G. Choi, K. Kim, and Y. Masuda, Sensors and Actuators B: Chemical, p. 132143, 2022; https://doi.org/10.1016/j.snb.2022.132143

[8] R. Blue and D. Uttamchandani, Measurement Science and Technology, vol. 28, no. 2, p. 022001, 2016; https://doi.org/10.1088/1361-6501/28/2/022001

[9] M. Boutamine, A. Bellel, S. Sahli, Y. Segui, and P. Raynaud, Thin Solid Films, vol. 552, pp. 196-203, 2014; https://doi.org/10.1016/j.tsf.2013.12.016

[10] J. Zhao et al., Sensors and Actuators B: Chemical, vol. 230, pp. 206-211, 2016; https://doi.org/10.1016/j.snb.2016.02.020

[11] U. Altenberend, A. Oprea, N. Barsan, and U. Weimar, Analytical and bioanalytical chemistry, vol. 405, no. 20, pp. 6445-6452, 2013; https://doi.org/10.1007/s00216-013-7023-x

[12] A. Botsialas, P. Oikonomou, D. Goustouridis, T. Ganetsos, I. Raptis, and M. Sanopoulou, Sensors and Actuators B: Chemical, vol. 177, pp. 776-784, 2013; https://doi.org/10.1016/j.snb.2012.11.050

[13] Z. Wang et al., Microelectronic Engineering, vol. 225, p. 111253, 2020; https://doi.org/10.1016/j.mee.2020.111253

[14] M. Hjiri, Journal of Materials Science: Materials in Electronics, vol. 31, no. 6, pp. 5025-5031, 2020; https://doi.org/10.1007/s10854-020-03069-4

[15] P. B. Koli, K. H. Kapadnis, U. G. Deshpande, U. J. Tupe, S. G. Shinde, and R. S. Ingale, Environmental Challenges, vol. 3, p. 100043, 2021; https://doi.org/10.1016/j.envc.2021.100043

[16] M. Babaei and N. Alizadeh, Sensors and Actuators B: Chemical, vol. 183, pp. 617-626, 2013; https://doi.org/10.1016/j.snb.2013.04.045

[17] V. Jousseaume, L. Favennec, A. Zenasni, and O. Gourhant, Surface and Coatings Technology, vol. 201, no. 22-23, pp. 9248-9251, 2007; https://doi.org/10.1016/j.surfcoat.2007.04.105

[18] V. Jousseaume et al., Sensors and Actuators B: Chemical, vol. 271, pp. 271-279, 2018; https://doi.org/10.1016/j.snb.2018.05.042

[19] F. Fanelli, S. Lovascio, R. d'Agostino, and F. Fracassi, Plasma Processes and Polymers, vol. 9, no. 11-12, pp. 1132-1143, 2012; https://doi.org/10.1002/ppap.201100157

[20] B. J. Brownlee, J. C. Claussen, and B. D. Iverson, ACS Applied Nano Materials, vol. 3, no. 10, pp. 10166-10175, 2020; https://doi.org/10.1021/acsanm.0c02121

[21] T. Santra, T. Bhattacharyya, F. Tseng, and T. Barik, AIP Advances, vol. 2, no. 2, p. 022132, 2012; https://doi.org/10.1063/1.4721654

[22] G. Borvon, A. Goullet, X. Mellhaoui, N. Charrouf, and A. Granier, Materials Science in Semiconductor Processing, vol. 5, no. 2-3, pp. 279-284, 2002; https://doi.org/10.1016/S1369-8001(02)00105-1

[23] J. El Sabahy, F. Ricoul, and V. Jousseaume, Microporous and Mesoporous Materials, vol. 330, p. 111560, 2022; https://doi.org/10.1016/j.micromeso.2021.111560

[24] V. Jousseaume, J. El Sabahy, C. Yeromonahos, G. Castellan, A. Bouamrani, and F. Ricoul, Microelectronic Engineering, vol. 167, pp. 69-79, 2017; https://doi.org/10.1016/j.mee.2016.10.003
[25] S. Partel, S. Kasemann, V. Matylitskaya, C. Thanner, C. Dincer, and G. Urban, Microelectronic Engineering, vol. 173, pp. 27-32, 2017; https://doi.org/10.1016/j.mee.2017.03.014
[26] A. S. de Freitas, C. C. Maciel, J. S. Rodrigues, R. P. Ribeiro, A. O. Delgado-Silva, and E. C. Rangel, Vacuum, vol. 194, p. 110556, 2021; https://doi.org/10.1016/j.vacuum.2021.110556
[27] M. Boutamine, O. Lezzar, A. Bellel, K. Aguir, S. Sahli, and P. Raynaud, Analytical Letters, vol. 51, no. 3, pp. 387-400, 2018; https://doi.org/10.1080/00032719.2017.1339356
[28] S. Partel, S. Kasemann, P. Choleva, C. Dincer, J. Kieninger, and G. A. Urban, Sensors and actuators B: chemical, vol. 205, pp. 193-198, 2014; https://doi.org/10.1016/j.snb.2014.08.065
[29] S. Zeinali, S. Homayoonnia, and G. Homayoonnia, Sensors and Actuators B: Chemical, vol. 278, pp. 153-164, 2019; https://doi.org/10.1016/j.snb.2018.07.006
[30] M. Jaritz, P. Alizadeh, S. Wilski, L. Kleines, and R. Dahlmann, Plasma Processes and Polymers, vol. 18, no. 8, p. 2100018, 2021; https://doi.org/10.1002/ppap.202100018
[31] M. Goujon, T. Belmonte, and G. Henrion, Surface and Coatings Technology, vol. 188, pp. 756-761, 2004; https://doi.org/10.1016/j.surfcoat.2004.07.048
[32] C. Zhang, J. Wyatt, S. Russell, and D. Weinkauf, Polymer, vol. 45, no. 22, pp. 7655-7663, 2004; https://doi.org/10.1016/j.polymer.2004.08.055
[33] I.-S. Bae et al., Progress in Organic Coatings, vol. 61, no. 2-4, pp. 245-248, 2008; https://doi.org/10.1016/j.porgcoat.2007.09.031
[34] J. Tang, E. Skotadis, S. Stathopoulos, V. Roussi, V. Tsouti, and D. Tsoukalas, Sensors and Actuators B: chemical, vol. 170, pp. 129-136, 2012; https://doi.org/10.1016/j.snb.2011.03.001
[35] L. Onsager, Journal of the American Chemical Society, vol. 58, no. 8, pp. 1486-1493, 1936; https://doi.org/10.1021/ja01299a050
[36] M. Filippidou, M. Chatzichristidi, and S. Chatzandroulis, Sensors and Actuators B: Chemical, vol. 284, pp. 7-12, 2019; https://doi.org/10.1016/j.snb.2018.12.095
[37] R. Igreja and C. Dias, Sensors and Actuators A: Physical, vol. 112, no. 2-3, pp. 291-301, 2004; https://doi.org/10.1016/j.sna.2004.01.040
[38] R. Igreja and C. Dias, Sensors and Actuators B: Chemical, vol. 115, no. 1, pp. 69-78, 2006; https://doi.org/10.1016/j.snb.2005.08.019
[39] P. Oikonomou et al., Microelectronic engineering, vol. 88, no. 8, pp. 2359-2363, 2011; https://doi.org/10.1016/j.mee.2011.02.085
[40] C. Sapsanis et al., Sensors, vol. 15, no. 8, pp. 18153-18166, 2015; https://doi.org/10.3390/s150818153
[41] T. Islam, A. Nimal, U. Mittal, and M. Sharma, Sensors and Actuators B: Chemical, vol. 221, pp. 357-364, 2015; https://doi.org/10.1016/j.snb.2015.06.101
[42] N. A. M. Safian et al., Sensors and Actuators B: Chemical, vol. 343, p. 130158, 2021; https://doi.org/10.1016/j.snb.2021.130158
[43] A. Fendri, R. Ramalingame, H. Ghariani, and O. Kanoun, 2017 14th International Multi-Conference on Systems, Signals & Devices (SSD), 2017, pp. 738-743: IEEE; https://doi.org/10.1109/SSD.2017.8167028